Turbulent nitrate fluxes in the Amundsen Gulf during ice-covered conditions

D. Bourgault,[1] C. Hamel,[2] F. Cyr,[1] J.-É. Tremblay,[3] P. S. Galbraith,[4] D. Dumont,[1] and Y. Gratton[5]

Received 28 April 2011; revised 21 June 2011; accepted 23 June 2011; published 2 August 2011.

[1] Turbulence and nitrate measurements collected in the Amundsen Gulf during ice-covered conditions in fall 2007 are combined to provide mean vertical profiles of eddy diffusivity $\overline{K}$ and diffusive nitrate fluxes $\overline{F}$. The mean diffusivity (with 95% confidence intervals) was maximum near the uppermost sampling depth (10 m) with $\overline{K}_{max}$ = 3(2, 5) × 10^{-3} m^2 s^{-1} and decreased exponentially to a depth of ~50 m, below which it was roughly constant at the background value $\overline{K}_b$ = 3(2, 5) × 10^{-6} m^2 s^{-1}. The nitracline, centered around 62 m depth, was subject to an eddy diffusivity close to the background value $\overline{K}_b$ and the mean diffusive nitrate flux across the nitracline was $\overline{F}_{nit}$ = 0.5(0.3, 0.8) mmol m^{-2} d^{-1}. These observations are compared with other regions and the role of vertical mixing on primary production in the Amundsen Gulf is discussed.
Citation: Bourgault, D., C. Hamel, F. Cyr, J.-É. Tremblay, P. S. Galbraith, D. Dumont, and Y. Gratton (2011), Turbulent nitrate fluxes in the Amundsen Gulf during ice-covered conditions, *Geophys. Res. Lett.*, *38*, L15602, doi:10.1029/2011GL047936.

1. Introduction

[2] Nutrient replenishment of the surface layer in the Amundsen Gulf occurs principally during ice-covered conditions (November to May), when primary production is at its minimum [*Tremblay et al.*, 2008]. Since nitrogen is the limiting element for primary producers in this region, the strength of its replenishment is thought to control overall annual productivity [*Tremblay and Gagnon*, 2009]. Nitrogen supply to the surface layer may come horizontally, from rivers and surrounding marginal seas, vertically, from upwellings and turbulent diffusion of nutrient-rich bottom layers [*Lewis et al.*, 1986], as well as from *in situ* biological processes such as ammonification and nitrification [*Tremblay et al.*, 2008]. While observations exist about the total contribution of these sources to nitrate uptake in the Amundsen Gulf [*Tremblay et al.*, 2008], little is known about each process taken separately. This is particularly true for the contribution of turbulent diffusion due to past difficulties of obtaining coincident turbulence and nitrate gradient measurements. While such observations now become more commonly available in ice-free environments (see references in Table 1), they are still rare in mobile ice-covered arctic environments.

[3] In 2007–2008, during the International Polar Year, a large multidisciplinary research initiative called the Circumpolar Flaw Lead (CFL) System Study was conducted to study the general oceanographic conditions in the Amundsen Gulf through an annual cycle [*Barber et al.*, 2010]. One novelty of the sampling strategy consisted in keeping the Canadian research ice-breaker *CCGS Amundsen* mobile throughout fall and winter in the Amundsen Gulf, in contrast to the overwintering fixed within the fast-ice of Franklin Bay during the Canadian Arctic Shelf Exchange Study (CASES) [*Fortier et al.*, 2008]. We synthesize here about five weeks of almost coincident turbulence and nitrate measurements collected during the CFL campaign to estimate the turbulent nitrate flux in the Amundsen Gulf during ice-covered conditions.

2. Sampling Conditions and Methods

[4] Measurements were collected aboard the *CCGS Amundsen* while drifting with large mobile ice floes in the Amundsen Gulf (Figure 1) between 16 November and 19 December, 2007, the year with the record-low ice cover minimum for the Arctic as a whole [*Maslanik et al.*, 2007]. The mean and standard deviation drift speed during sampling was 0.08 ± 0.07 m s^{-1}, according to GPS records. During the sampling period ice coverage was greater than 90% and made principally of first-year ice, 2–10 km wide vast floes, 50 to 70 cm thick (Canadian Ice Service, Environment Canada, http://ice-glaces.ec.gc.ca/).

[5] Dissipation rates of turbulent kinetic energy ϵ (in W kg^{-1}) were calculated as $\epsilon = (15/2)\nu\langle u_z^2\rangle$, where ν is kinematic viscosity and u_z is the microscale (~cm) vertical shear [e.g., *Sundfjord et al.*, 2007; *Martin et al.*, 2010; *Schafstall et al.*, 2010]. The latter is measured with an airfoil shear probe SPM-38-1 and pressure sensor mounted on a loosely-tethered free-fall vertical microstructure profiler (VMP-500) manufactured by Rockland Scientific International. The $\langle\ \rangle$ symbol represents 4-m scale averaging with instrumental noise removed prior to averaging. Such dissipation measurements are generally accepted to be accurate to within a factor of 2 [*Oakey*, 1982]. The VMP is also equipped with SeaBird SBE-3F and SBE-4C sensors for fine-scale (~dm) *T-S* measurements from which the density ρ is calculated using the equation of state of seawater. The VMP was deployed through the *CCGS Amundsen* moon pool. Since the ship draft is 7.18 m, the top 10 m of profiles are discarded from the analysis to avoid ship contamination.

[1]Institut des Sciences de le Mer de Rimouski, Université du Québec à Rimouski, Rimouski, Quebec, Canada.
[2]Département de Physique, Université de Sherbrooke, Sherbrooke, Quebec, Canada.
[3]Département de Biologie, Université Laval, Quebec, Quebec, Canada.
[4]Maurice Lamontagne Institute, Fisheries and Oceans Canada, Mont-Joli, Quebec, Canada.
[5]Centre Eau Terre Environnement, Quebec, Quebec, Canada.

0094-8276/11/2011GL047936

Table 1. Comparisons of Nitrate Turbulent Fluxes Reported in the Literature From Different Regions of the World Ocean[a]

Reference	Region	$\overline{F}$ (mmol m^{-2} d^{-1})
Martin et al. [2010]	Porcupine Abyssal Plain	0.09
Horne et al. [1996]	Georges Bank	0.047–0.18
Lewis et al. [1986]	Subtropical North Atlantic	0.14
Law et al. [2003]	Antarctic Circumpolar Current	0.17
This study	Amundsen Gulf (>90% i.c.)	0.5
Carr et al. [1995]	Equatorial Pacific	0.1–1
Sundfjord et al. [2007]	Barents Sea (40–90% i.c.)	0.1–2
Rippeth et al. [2009]	Irish Sea	1.5
Law et al. [2001]	Northern North Atlantic	1.8
Sharples et al. [2007]	Celtic Sea Shelf Edge	1.3–3.5
Hales et al. [2009]	New England Shelf Break	0.8–5
Hales et al. [2005]	Oregon shelf	$\mathcal{O}(10^1)$
Sharples et al. [2001]	New Zealand Shelf	12
Schafstall et al. [2010]	Mauritanian Upwelling Region	120

[a]The values reported may represent, depending on studies, the flux through the nitracline, through the base of the euphotic zone or through the base of the mixed layer. Values are sorted from lowest to highest. A molar mass of 62 g mol^{-1} was used for converting nitrate concentration from mg to mmol as used in some of the references listed. The abbreviation i.c. stands for ice coverage.

[6] The turbulent diffusivity of nitrate was calculated as $K = \Gamma\epsilon/N^2$ [*Osborn*, 1980], with $\Gamma = 0.2$, $N^2 = -(g/\rho)\rho_z$ and $g = 9.8$ m^2 s^{-1} [e.g., *Sharples et al.*, 2007; *Rippeth et al.*, 2009; *Martin et al.*, 2010; *Schafstall et al.*, 2010]. Note that although this model for K was initially derived for shear mixing it has proven adequate by *Sundfjord et al.* [2007, Figure 12] in a similar ice-covered coastal arctic environment (Barents Sea) where double-diffusion mixing may have been present. Furthermore, the *Kelley* [1990] parameterization for double-diffusion of salt applied to our CTD data suggests that double-diffusion mixing was negligible in the Amundsen Gulf during the sampling period (not shown).

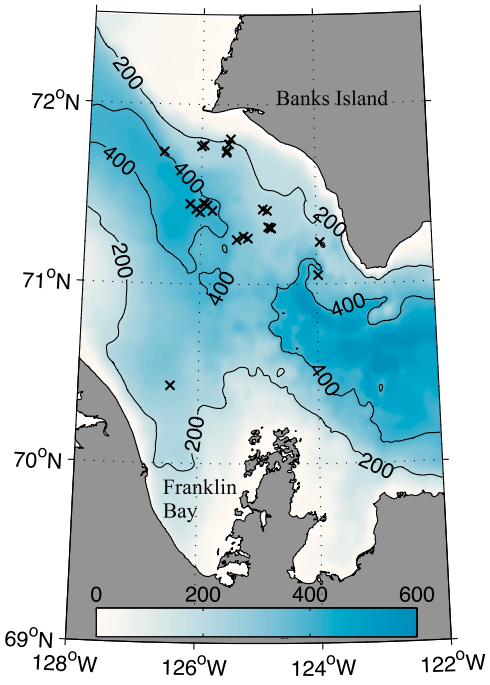

Figure 1. Map and bathymetry (m) of the Amundsen Gulf and positions of the 26 stations where turbulence and nitrate profiles were collected in November–December 2007.

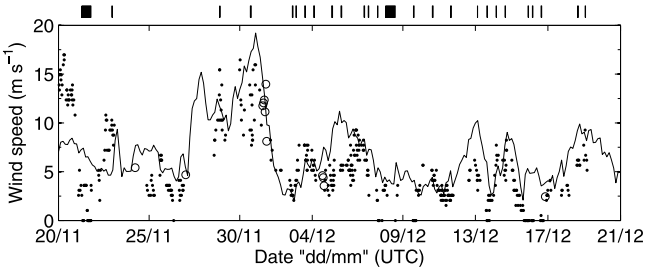

Figure 2. Wind speed observations in the Amundsen Gulf during the sampling period. NCEP-NARR reanalysis (solid curve), *CCGS Amundsen* navigation anemometer reported in the science log book during sampling operations (black dots), and meteorological science station aboard the *CCGS Amundsen* (circles). The black lines at the top indicate the sampling periods reported here.

[7] Overall, 175 VMP profiles collected at 26 different stations within the Amundsen Gulf were used in the analysis (Figure 1). Generally, four consecutive VMP profiles were collected at every station except for two where 55 and 24 profiles were collected. Sampling periods roughly spanned the range of wind speed conditions occurring during the 5-week survey period presented here (Figure 2) with a slight bias towards low wind conditions; the mean wind speed during turbulence sampling was 80% of the mean occurring during the entire survey.

[8] Nitrate (NO_3^-) concentrations $\mathcal{N}$ (in mmol m^{-3}) were measured with a Satlantic Isus V3 nitrate sensor fixed underneath a rosette sampler. At some stations, bottle samples were also collected and nitrate concentration determined from laboratory analyses as detailed by *Tremblay et al.* [2008]. The Isus sensor measurements were then post-calibrated by linear regression against 151 samples from 12 stations. The calibration yielded a correlation coefficient $R = 0.91$ and a standard error ±2.2 mmol m^{-3} (P. Guillot, Québec-Océan, personal communication, 2011), consistent with the manufacturer accuracy specification of ±2 mmol m^{-3}. The minimum concentration that could be detected with this sensor is 0.5 mmol m^{-3}. The measurements were then averaged into 4-m bins matching the dissipation rate data. Figure 3 shows a typical 4-m scale calibrated profile compared with bottled samples. Although the Isus sensor is characterized by some systematic deviations relative to the bottle profile, it captures satisfactorily well the position and strength of the nitracline, which is essential for the analysis presented here, with around 15% difference in its maximum gradient and 10% difference in its position as defined by the maximum gradient. Note also that very low concentrations (<0.5 mmol m^{-3}) near the surface (10–20 m, Figure 3) are below the reliable detection capacity of the Isus sensor. Overall, 71 nitrate profiles were grouped and averaged per station, providing 26 nitrate profiles.

[9] Profiles of vertical turbulent nitrate fluxes (in mmol m^{-2} d^{-1}) were calculated by combining VMP and nitrate observations through $F = -K\mathcal{N}_z \times 86\,400$ s d^{-1}. Each of the 175 K profiles was associated with the closest of the 26 nitrate profiles, providing 175 profiles of nitrate fluxes F.

[10] Measurements were synthesized into averaged profiles considered to be representative of conditions prevailing in the Amundsen Gulf throughout the sampling period. As

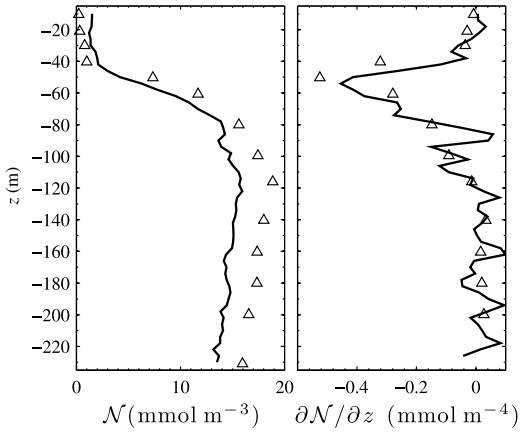

Figure 3. Example of (left) a typical nitrate profile and (right) its gradient (3 December 2007). The triangles represent measurements from laboratory analyses of bottled water samples and the solid lines represent the 4-m scale calibrated Isus-V3 sensor measurements.

recommended by *Baker and Gibson* [1987], the mean ($\overline{X}$) of small data sets (10–100 samples) of turbulence variables that are approximately lognormally distributed in the ocean, such as ϵ and K, was estimated using the maximum likelihood estimator $\overline{X} = \exp(m + s^2/2)$, where m and s^2 are the arithmetic mean and variance of $\ln(X)$, respectively. The mean of other variables ($\overline{N^2}$, $\overline{\mathcal{N}}$, $\overline{F}$) was estimated using the standard arithmetic mean.

[11] Ninety-five percent confidence intervals on means were determined by bootstrap analysis. Unless otherwise specified the numbers in parentheses provided next to mean values represent the lower 2.5% and upper 97.5% confidence intervals on the mean. For symmetric confidence intervals the symbol ± is used.

3. Observations

[12] On average over the sampling period and region, nitrate concentrations exhibited a two-layer structure with minimum concentration of $\overline{\mathcal{N}}_{\min} = 2.7 \pm 0.5$ mmol m^{-3} near the surface (10–20 m) and maximum $\overline{\mathcal{N}}_{\max} = 15.6 \pm 0.5$ mmol m^{-3} at 150 m depth (Figure 4). Note however that very low concentration near the sea surface were not captured reliably with the Isus sensor (see section 2 and Figure 3) and bottled samples rather average to $\overline{\mathcal{N}}^{\text{bot}}_{\min} = 0.5 \pm 0.3$ mmol m^{-3}. The mean position, and standard deviation, of the nitracline was $\overline{z}_{\text{nit}} = -62 \pm 12$ m, which is roughly 15 m below the pycnocline (Figure 4), and was characterized with a mean gradient $(\overline{\mathcal{N}_z})_{\text{nit}} = -2.0 \pm 0.1$ mmol m^{-4}.

[13] Mean dissipation rates of turbulent kinetic energy were maximum at 10 m depth with $\overline{\epsilon}_{\max} = 4.3(2.6, 7.3) \times 10^{-7}$ W kg^{-1} and decreased approximately exponentially with depth to the minimum value $\overline{\epsilon}_{\min} = 1.5(1.1, 2.1) \times 10^{-9}$ W kg^{-1} around 100 m (Figure 4). Note that the gray zones in Figure 4 show confidence intervals on the means and thus provide no information on the variability. The dissipation rate varies by 5 orders of magnitude at 10-m depth and are lognormally distributed in the range 10^{-10}–10^{-5} W kg^{-1}. At greater depth (>50 m) the variability spans about 3 orders of magnitude in the range 10^{-10}–10^{-7} W kg^{-1}.

[14] Eddy diffusivity was maximum at 10 m, with $\overline{K}_{\max} = 5(3, 9) \times 10^{-3}$ m^2 s^{-1}, and decayed exponentially to about 50 m depth, below which it stayed approximately constant down to 150 m (Figure 4). A least squares fit with bootstrapped 95% confidence intervals yielded the following piecewise analytical function for the depth-dependance of the mean eddy diffusivity:

$$\overline{K}(z) = \begin{cases} \overline{K}_0 e^{\delta z} & \text{for } -46 \le z \le -10 \text{ m} \\ \overline{K}_b & \text{for } -150 \le z < -46 \text{ m,} \end{cases} \quad (1)$$

with $\overline{K}_0 = 1.1(0.7, 1.8) \times 10^{-2}$ m^2 s^{-1}, $\delta = 0.17 \pm 0.02$ m^{-1} and $\overline{K}_b = 3.4(2.3, 5.1) \times 10^{-6}$ m^2 s^{-1} (Figure 4). The nitracline, being typically located at a greater depth than 46 m, was therefore subject to an eddy diffusivity close to the background value $\overline{K}_b$.

[15] The mean nitrate turbulent diffusive flux was in the range $-4 < \overline{F} < 6$ mmol m^{-2} d^{-1} throughout the profile (Figure 4). Through the nitracline it was $\overline{F}_{\text{nit}} = 0.5(0.3, 0.8)$ mmol m^{-2} d^{-1}.

4. Discussion

[16] In comparison to other estimates available throughout the world ocean, the mean turbulent nitrate flux reported here for the Amundsen Gulf during ice-covered conditions

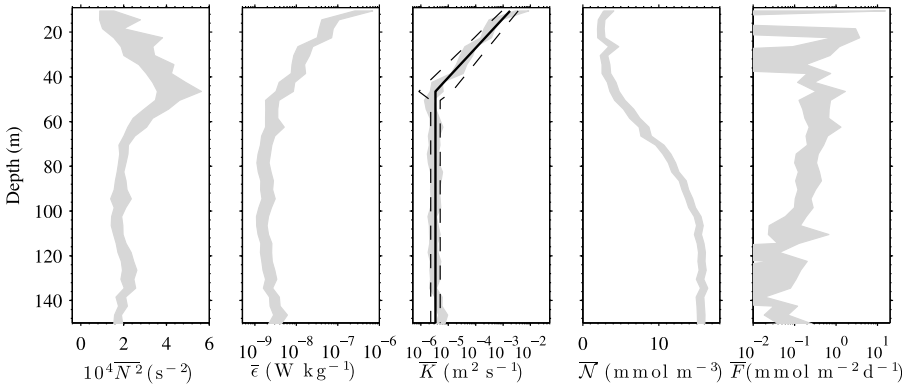

Figure 4. Averages of buoyancy frequency squared $\overline{N^2}$, dissipation rate $\overline{\epsilon}$, eddy diffusivity $\overline{K}$, nitrate concentration $\overline{\mathcal{N}}$ and vertical nitrate flux $\overline{F}$ for the Amundsen Gulf. Gray shadows are 95% confidence intervals. Only positive values greater than 10^{-2} mmol m^{-2} d^{-1} of nitrate fluxes are presented. The black solid line in the third plot is the best fit provided by equation (1) along with the 95% confidence intervals (dashed lines). Note that the depth scale starts at 9 m.

is comparable, in terms of order of magnitude, to most ice-free offshore ocean regions such as the Porcupine Abyssal Plain, the Northern North Atlantic, the Southern Ocean or the Equatorial Pacific as well as to the ice-covered Barents Sea (Table 1). On the other hand, this mean flux is about an order of magnitude smaller than values reported for more energetic environments like shelves, and two orders of magnitude smaller compared to the Mauritanian upwelling region (Table 1).

[17] While some of the studies listed in Table 1 concluded that vertical turbulent mixing may dominate nitrate uptake in surface layers and may control the net community productivity [e.g., *Lewis et al.*, 1986; *Sharples et al.*, 2007; *Hales et al.*, 2009; *Rippeth et al.*, 2009], other studies have reached opposite conclusions. For example, while *Schafstall et al.* [2010] reported one of the highest turbulent nitrate flux to date (Table 1), they concluded that it only represented 10%–25% of what was required to support the net community production along the Mauritanian Upwelling Region. They suggested that vertical advection and lateral eddy fluxes may provide the missing nitrate supply. Similarly, *Martin et al.* [2010] concluded that vertical mixing contributed little (about 2%) to the total nitrate uptake in the euphotic zone in the Porcupine Abyssal Plain. They considered other physical processes, such as those associated with mesoscale phenomena, but also hypothesized that biological nitrification could provide as much, or perhaps even more, nitrate to the euphotic zone than turbulent mixing.

[18] Returning to the context of the Amundsen Gulf of fall 2007, we found that the total rate of nitrate supply above the nitracline was $\overline{\mathcal{N}_t^{\mathrm{tot}}} = 14.6 \pm 2.7$ μmol m^{-3} d^{-1}, as determined from a linear fit to 8 groups of bottle samples collected from 5 November 2007 to 9 January 2008 (not shown but with $R^2 = 0.81$, $p < 0.001$ and following *Tremblay et al.* [2008]).

[19] The contribution from turbulent mixing to this rate could be estimated by dividing the turbulent flux through the nitracline F_{nit} by the thickness of the nitracline $|z_{\mathrm{nit}}|$ and averaging over all samples. This gives $\overline{\mathcal{N}_t} = \overline{F_{\mathrm{nit}}/|z_{\mathrm{nit}}|} = 9(5, 14)$ μmol m^{-3} d^{-1} from turbulent diffusion alone. Comparing these values (i.e. $\overline{\mathcal{N}_t}/\overline{\mathcal{N}_t^{\mathrm{tot}}}$) suggests that turbulent mixing contributed on average to 60% of the total nitrate uptake in the Amundsen Gulf during fall 2007.

[20] This conclusion contrasts with that of *Tremblay et al.* [2008] who hypothesized that vertical mixing contributed little, compared to nitrification processes, to nitrate uptake under the immobile landfast ice of Franklin Bay (Figure 1) during fall-winter 2003/04. However, we note that the nitracline in Franklin Bay during fall-winter 2003/04 was up to an order of magnitude weaker than during fall 2007 with gradients in the range $-0.4 \leq (\mathcal{N}_z)_{\mathrm{nit}} \leq -0.2$ mmol m^{-4} (determined from *Tremblay et al.* [2008, Figure 3]), compared to $(\overline{\mathcal{N}_z})_{\mathrm{nit}} = -2.0 \pm 0.1$ mmol m^{-4} for fall 2007. Assuming that the nitracline in 2003 was subject to the same background diffusivity as in 2007 of $\overline{K_b} = 3.4 \times 10^{-6}$ m^2 s^{-1} and letting the nitracline depth to be 40 m during fall 2003 [*Tremblay et al.*, 2008] yields $(\overline{\mathcal{N}_t})_{03} = -[\overline{K_b}\,(\mathcal{N}_z)_{\mathrm{nit}}/40\ \mathrm{m}] \times 86\,400$ s d^{-1} = 1 to 3 μmol m^{-3} d^{-1}, from turbulent diffusion alone. Comparing this with the total rate reported by *Tremblay et al.* [2008] for fall 2003 of $(\overline{\mathcal{N}_t^{\mathrm{tot}}})_{03} = 13.2 \pm 2.5$ μmol m^{-3} d^{-1} suggests that 8% to 20% of the nitrate supply in 2003 may have been from vertical turbulent diffusion. This supports *Tremblay et al.*'s [2008] hypothesis that renewal of nitrate from vertical mixing in fall 2003 in Franklin Bay may not have been the dominant mechanism.

5. Conclusions

[21] Our observations show that while the surface layer may be subject to large diffusivities, the nitracline is essentially subject to the low background diffusivity $\overline{K_b}$. For two-layer models where the interface is set around the nitracline, or the pycnocline [e.g., *Shadwick et al.*, 2011], it appears reasonable to use a constant background diffusivity $\overline{K_b}$ to model turbulent diffusive fluxes of tracers across the layers. However, if mean turbulent diffusivity is needed within the surface layer [e.g., *Else et al.*, 2011] the empirical relationship given by equation (1) is proposed.

[22] Our analysis supports the conclusion of *Tremblay et al.* [2008] that turbulent diffusion may have played a secondary role in nitrate uptake in Franklin Bay in 2003. However, we reached an opposite conclusion for the Amundsen Gulf for fall 2007 where 60% of total nitrate supply may have come from turbulent diffusion. It is unclear at this point whether these opposite conclusions were reached because we are comparing two different regions or years. However, the observations presented here provide a source for testing sea ice-ocean-biological models [e.g., *Lavoie et al.*, 2009] from which insights regarding the functioning of the coastal arctic ecosystem in a changing climate could be gained. Such model assessments against field measurements are critically needed because turbulence parameterization remains one of the greatest uncertainties in climate prediction. The information provided here may help to progress rapidly in that direction.

[23] **Acknowledgments.** This component of the CFL program was funded by the Canadian International Polar Year (IPY) program office, the Natural Sciences and Engineering Research Council (NSERC), and the Canada Foundation for Innovation (CFI) and is a contribution to the scientific program of Québec-Océan. Thanks to Pascal Guillot for processing the nitrate data, Matthew Asplin and Brent Else for providing us with GPS and wind data and Dan Kelley for fruitful discussion on statistics and double-diffusion.

[24] The Editor wishes to acknowledge Tom Rippeth and an anonymous reviewer for their assistance in evaluating this paper.

References

Baker, M. A., and C. H. Gibson (1987), Sampling turbulence in the stratified ocean: Statistical consequences of strong intermittency, *J. Phys. Oceanogr.*, *17*, 1817–1836.

Barber, D. G., M. G. Asplin, Y. Gratton, J. Lukovich, R. J. Galley, R. L. Raddatz, and D. Leitch (2010), The International Polar Year (IPY) Circumpolar Flaw Lead (CFL) System Study: Overview and the physical system, *Atmos. Ocean*, *48*(4), 225–243, doi:10.3137/OC317.2010.

Carr, M.-E., M. R. Lewis, and D. Kelley (1995), A physical estimate of new production in the equatorial Pacific along 150°W, *Limnol. Oceanogr.*, *40*, 138–147.

Else, B. G. T., T. N. Papakyriakou, R. J. Galley, W. M. Drennan, L. A. Miller, and H. Thomas (2011), Wintertime CO_2 fluxes in an arctic polynya using eddy covariance: Evidence for enhanced air-sea gas transfer during ice formation, *J. Geophys. Res.*, doi:10.1029/2010JC006760, in press.

Fortier, L., D. Barber, and J. Michaud (Eds.) (2008), *On Thin Ice: A Synthesis of the Canadian Arctic Shelf Exchange Study* (*CASES*), 219 pp., Aboriginal Issues, Winnipeg, Manitoba, Canada.

Hales, B., J. N. Moum, P. Covert, and A. Perlin (2005), Irreversible nitrate fluxes due to turbulent mixing in a coastal upwelling system, *J. Geophys. Res.*, *110*, C10S11, doi:10.1029/2004JC002685.

Hales, B., D. Hebert, and J. Marra (2009), Turbulent supply of nutrients to phytoplankton at the New England shelf break front, *J. Geophys. Res.*, *114*, C05010, doi:10.1029/2008JC005011.

Horne, E. P. W., J. W. Loder, C. E. Naimie, and N. S. Oakey (1996), Turbulence dissipation rates and nitrate supply in the upper water column on Georges Bank, *Deep Sea Res., Part II*, *43*, 1683–1712.

Kelley, D. E. (1990), Fluxes through diffusive staircases: A new formulation, *J. Geophys. Res.*, *95*(C3), 3365–3371.

Lavoie, D., R. W. Macdonald, and K. L. Denman (2009), Primary productivity and export fluxes on the Canadian shelf of the Beaufort Sea: A modelling study, *J. Mar. Syst.*, *75*, 17–32, doi:10.1016/j.jmarsys.2008.07.007.

Law, C., A. Martin, M. Liddicoat, A. Watson, K. Richards, and E. Woodward (2001), A Lagrangian SF6 tracer study of an anticyclonic eddy in the North Atlantic: Patch evolution, vertical mixing and nutrient supply to the mixed layer, *Deep Sea Res., Part II*, *48*, 705–724, doi:10.1016/S0967-0645(00)00112-0.

Law, C., E. Abraham, A. Watson, and M. Liddicoat (2003), Vertical eddy diffusion and nutrient supply to the surface mixed layer of the Antarctic Circumpolar Current, *J. Geophys. Res.*, *108*(C8), 3272, doi:10.1029/2002JC001604.

Lewis, M. R., W. G. Harrison, N. S. Oakey, D. Hebert, and T. Plat (1986), Vertical nitrate fluxes in the oligotrophic ocean, *Science*, *234*, 870–873.

Martin, A. P., M. I. Lucas, S. C. Painter, R. Pidcock, H. Prandke, H. Prandke, and M. C. Stinchcombe (2010), The supply of nutrients due to vertical turbulent mixing: A study at the Porcupine Abyssal Plain study site in the northeast Atlantic, *Deep Sea Res., Part II*, *57*, 1293–1302, doi:10.1016/j.dsr2.2010.01.006.

Maslanik, J. A., C. Fowler, J. Stroeve, S. Drobot, J. Zwally, D. Yi, and W. Emery (2007), A younger, thinner arctic ice cover: Increased potential for rapid, extensive sea-ice loss, *Geophys. Res. Lett.*, *34*, L24501, doi:10.1029/2007GL032043.

Oakey, N. S. (1982), Determination of the rate of dissipation of turbulent energy from simultaneous temperature and velocity shear microstructure measurements, *J. Phys. Oceanogr.*, *12*, 256–271.

Osborn, T. R. (1980), Estimates of the local rate of vertical diffusion from dissipation measurements, *J. Phys. Oceanogr.*, *10*, 83–89.

Rippeth, T. P., P. Wiles, M. R. Palmer, J. Sharples, and J. Tweddle (2009), The diapcynal nutrient flux and shear-induced diapcynal mixing in the seasonally stratified western Irish Sea, *Cont. Shelf Res.*, *29*, 1580–1587.

Schafstall, J., M. Dengler, P. Brandt, and H. Bange (2010), Tidal-induced mixing and diapycnal nutrient fluxes in the Mauritanian upwelling region, *J. Geophys. Res.*, *115*, C10014, doi:10.1029/2009JC005940.

Shadwick, E. H., et al. (2011), Seasonal variability of the inorganic carbon system in the Amundsen Gulf region of the southeastern Beaufort Sea, *Limnol. Oceanogr.*, *56*, 303–322, doi:10.4319/lo.2011.56.1.0303.

Sharples, J., C. M. Moore, and E. R. Abraham (2001), Internal tide dissipation, mixing, and vertical nitrate flux at the shelf edge of NE New Zealand, *J. Geophys. Res.*, *106*(C7), 14,069–14,081.

Sharples, J., et al. (2007), Spring-neap modulation of internal tide mixing and vertical nitrate fluxes at a shelf edge in summer, *Limnol. Oceanogr.*, *52*, 1735–1747.

Sundfjord, A., I. Fer, Y. Kasajima, and H. Svendsen (2007), Observations of turbulent mixing and hydrography in the marginal ice zone of the Barents Sea, *J. Geophys. Res.*, *112*, C05008, doi:10.1029/2006JC003524.

Tremblay, J.-É., and J. Gagnon (2009), The effects of irradiance and nutrient supply on the productivity of arctic waters: A perspective on climate change, in *Influence of Climate Change on the Changing Arctic and Sub-arctic Conditions*, edited by J. C. J. Nihoul and A. G. Kostianoy, pp. 73–93, Springer, Dordrecht, Netherlands, doi:10.1007/978-1-4020-9460-6_7.

Tremblay, J.-É., K. Simpson, J. Martin, L. Miller, Y. Gratton, D. Barber, and N. M. Price (2008), Vertical stability and the annual dynamics of nutrients and chlorophyll fluorescence in the coastal, southeast Beaufort Sea, *J. Geophys. Res.*, *113*, C07S90, doi:10.1029/2007JC004547.

D. Bourgault, F. Cyr, and D. Dumont, Institut des Sciences de le Mer de Rimouski, Université du Québec à Rimouski, 310, Allée des Ursulines, CP 3300, Rimouski, QC G5L 3A1, Canada. (daniel_bourgault@uqar.ca)

P. S. Galbraith, Maurice Lamontagne Institute, Fisheries and Oceans Canada, 850 route de la Mer, Mont-Joli, QC G5H 3Z4, Canada.

Y. Gratton, Centre Eau Terre Environnement, 490 de la Couronne, Québec, QC G1K 9A9, Canada.

C. Hamel, Département de Physique, Université de Sherbrooke, Sherbrooke, QC J1K 2R1, Canada.

J.-É. Tremblay, Département de Biologie, Université Laval, Pavillon Alexandre-Vachon, Québec, QC G1V 0A6, Canada.